Supporting Information

Shape-Controlled Synthesis of Hybrid Nanomaterials via Three-Dimensional Hydrodynamic Focusing Method

Mengqian Lu,[1] Shikuan Yang,[1] Yi-Ping Ho,[2,3] Christopher L. Grigsby,[2] Kam W. Leong,[2] and Tony Jun Huang[1*]*

[1] Department of Engineering Science and Mechanics, The Pennsylvania State University, University Park, Pennsylvania 16802, United States

[2] Department of Biomedical Engineering, Duke University, Durham, North Carolina 27708, United States

[3] Interdisciplinary Nanoscience Center (iNANO), Aarhus University, 8000 Aarhus C, Denmark

* Address correspondence to kam.leong@duke.edu and junhuang@psu.edu

TTF-Au Hybrid Materials Synthesized by 3D-HF Method

Fig. S1 to Fig. S6 are SEM images of TTF-Au hybrid materials synthesized by 3D-HF methods, with larger scale than those in Fig. 2 to show more structures in one image.

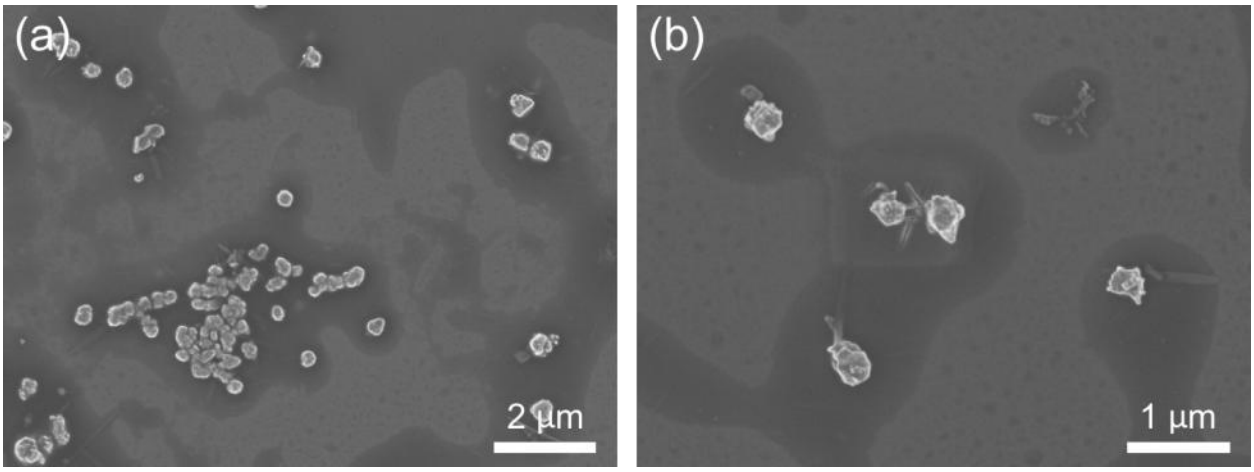

Figure S1. SEM images of the resulting materials formed at the flow rate ratio of 20.

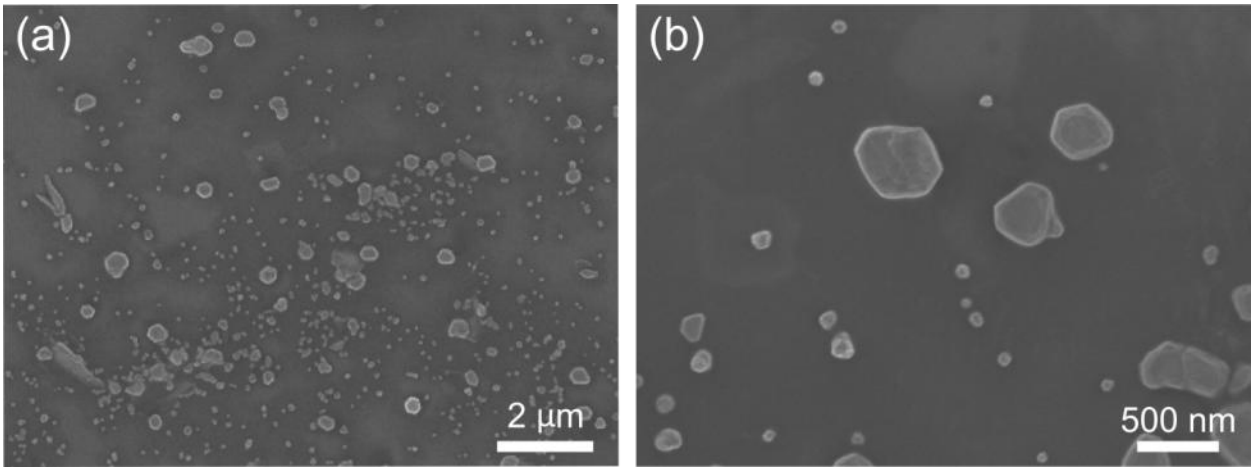

Figure S2. SEM images of the resulting materials formed at the flow rate ratio of 10.

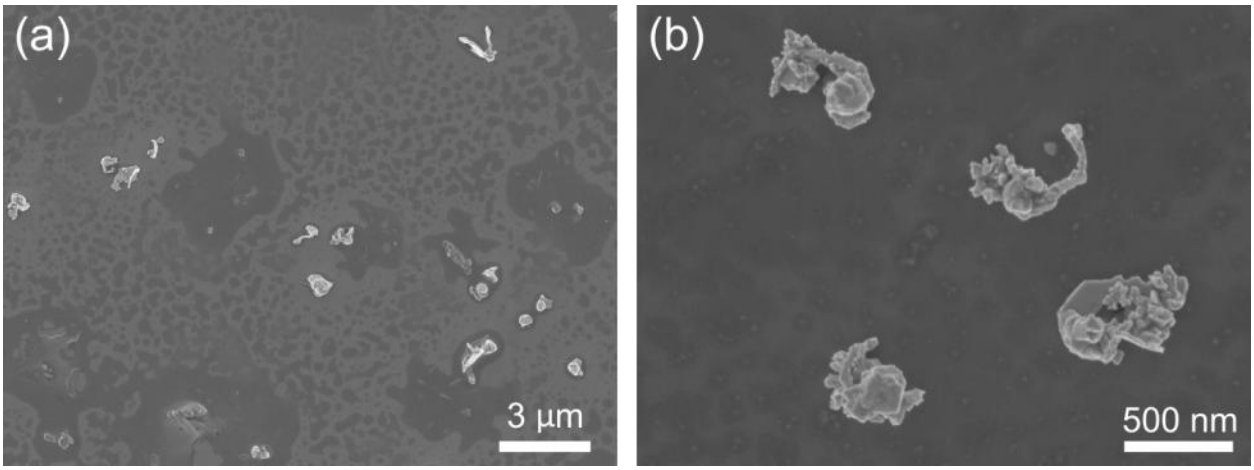

Figure S3. SEM images of the resulting materials formed at the flow rate ratio of 5.

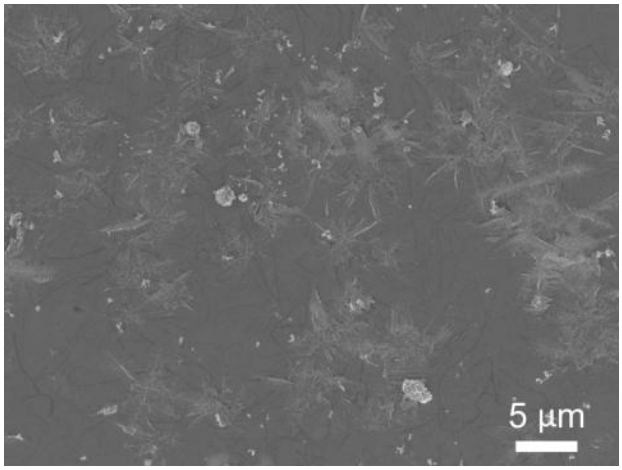

Figure S4. SEM images of the resulting materials formed at the flow rate ratio of 2.

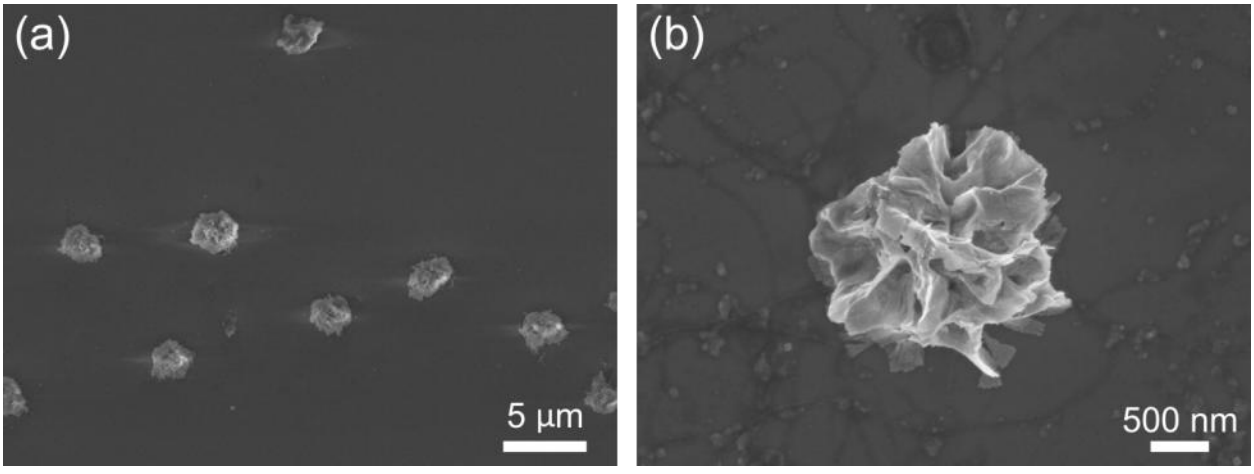

Figure S5. SEM images of the resulting materials formed at the flow rate ratio of 0.5.

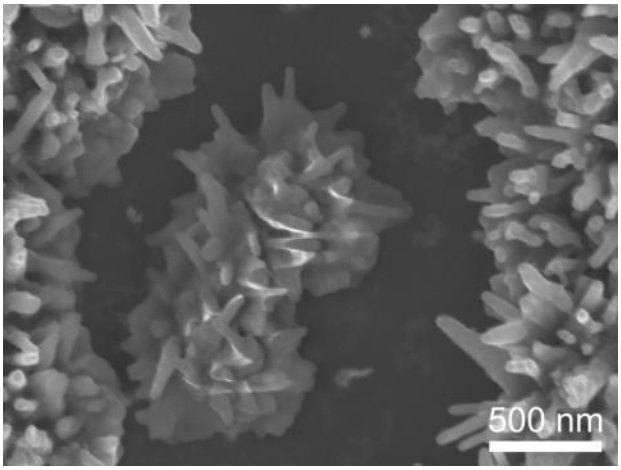

Figure S6. SEM images of the resulting materials formed at the flow rate ratio of 0.2.

Shear Stress Calculation

The shear stress (σ) can be calculated by the equation: $\sigma = \mu \cdot \partial v/\partial x$, where v is the flow velocity, x is the distance from the channel wall, and μ is the dynamic viscosity of the fluid. The velocity distribution was simulated using a computational fluid dynamic (CFD) simulation software (CFD-ACE+, ESI-CFD), as shown in Fig. S7. The highest shear rate ($\dot{\gamma} = \partial v/\partial x$) within the reaction zone was calculated as 1.1 $\times 10^4$ s^{-1}. We used the viscosity of acetonitrile at room temperature (0.3410 $\times 10^{-3}$ Pa·s) for the shear stress calculation. The highest shear rate within the reaction zone was then calculated as 3.75 Pa.

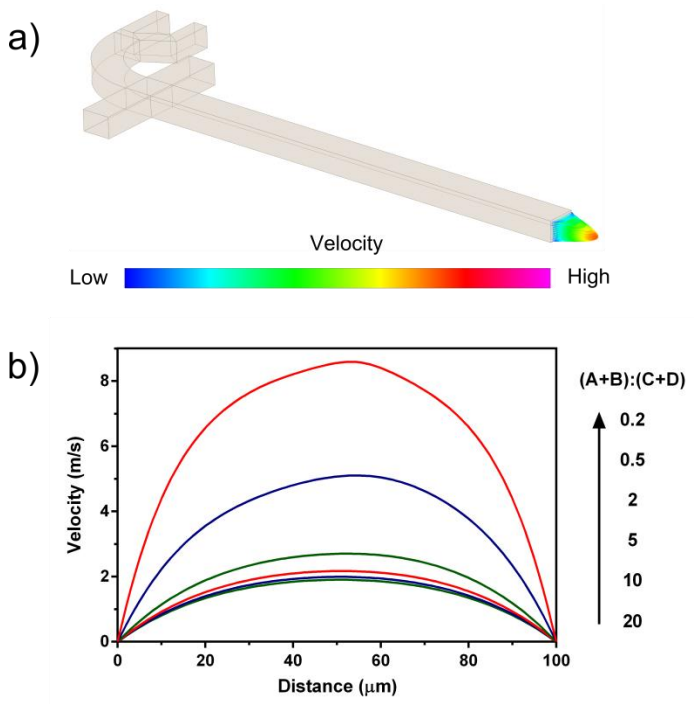

Figure S7. (a) The velocity distribution of fluid velocity in the cross-section of the microfluidic channel. (b) The velocity distribution at the center line in the cross-section in (a).

TTF-Au Hybrid Materials Synthesized by the Bulk Mixing Method

By changing the feed molar ratio of TTF/$HAuCl_4$, the TTF-Au hybrid materials synthesized by the bulk mixing method show morphological changes, as shown in Fig. S8 and Fig. S9. These morphological changes follow the same trend as predicted by the formation mechanism, and are similar to the morphological changes in the 3D-HF case in Fig. 2 and Fig. 3.

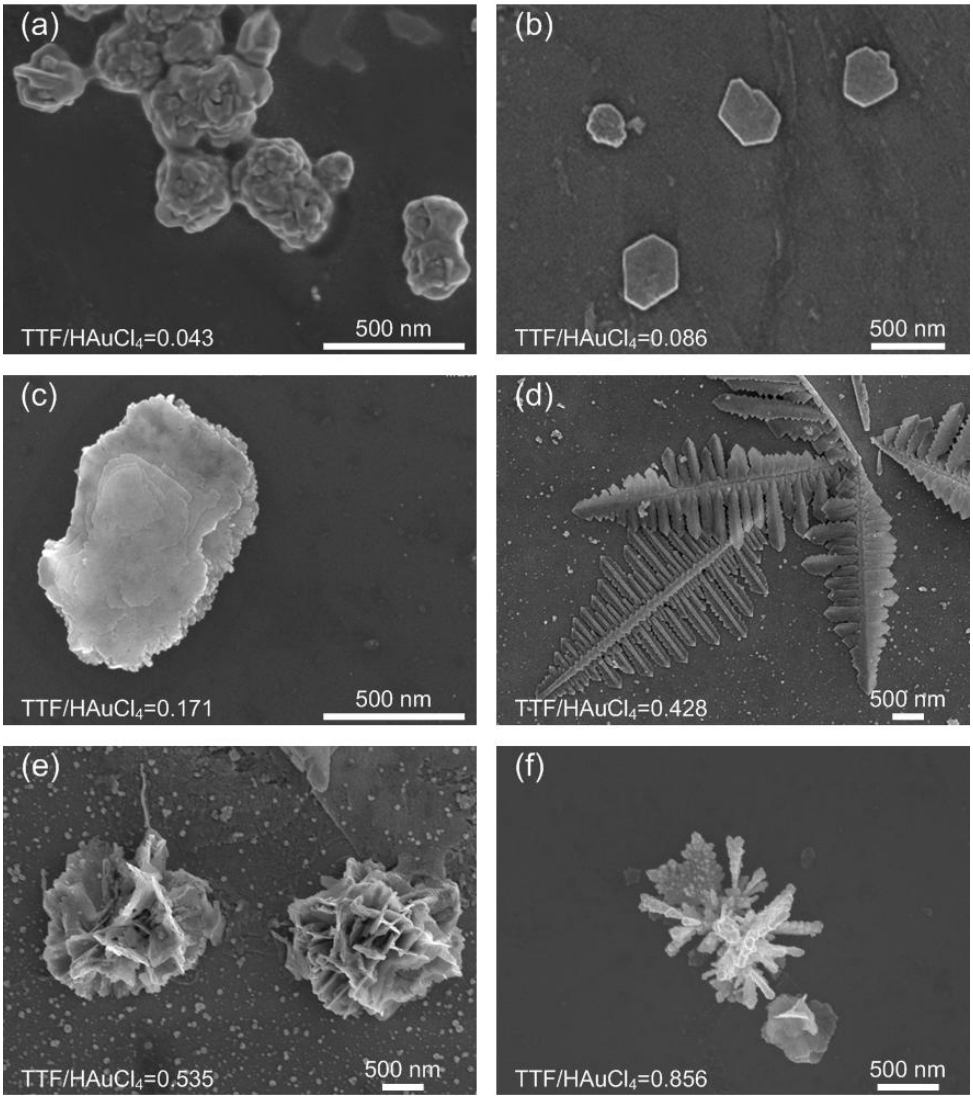

Figure S8. SEM images of nanomaterials prepared using the bulk mixing method with feed molar ratio of $TTF/HAuCl_4$ at the range between 0.043 and 0.856. As the feed molar ratio of $TTF/HAuCl_4$ increased, the morphologies of the synthesized nanomaterials experienced changes through (a) branching aggregates consisting of irregularly aligned polyhedral crystals, (b) triangle or hexagonal shape, (c) multi-layered structures consisting of thin and flat layers, (d) two-dimensional dendritic nanostructures, (e) flower-like aggregates consisting of thin, flat petals, and (f) coral-like aggregates consisting of fibers.

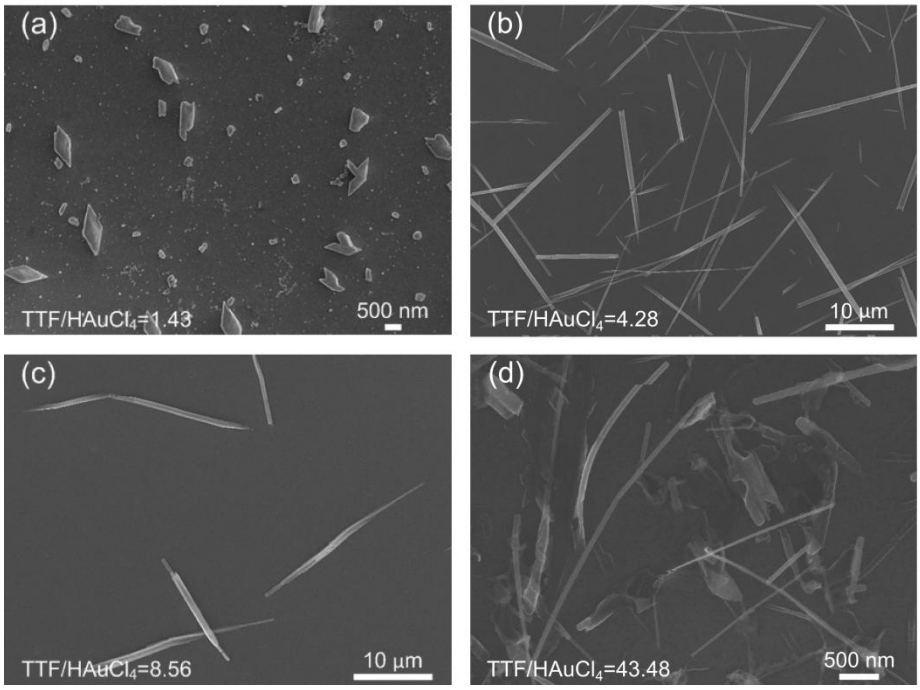

Figure S9. SEM images of nanomaterials prepared using the bulk mixing method with feed molar ratio of TTF/$HAuCl_4$ at the range between 1.43 and 43.48. As the feed molar ratio of TTF/$HAuCl_4$ increased, the morphologies of the synthesized nanomaterials experienced changes through (a) diamond shape with apex angle of 58º, (b) long wires of several tens of micrometers, (c) wires of ~10 micrometers, and (d) wires of 3-5 micrometers.

XRD Pattern of Structures Formed at Different Molar Ratio of TTF/$HAuCl_4$

The nanostructures synthesized by the bulk mixing method at different molar ratio of TTF/$HAuCl_4$ were characterized by x-ray diffraction (XRD), as shown in Fig. S10. The value of the distance (d) between adjacent (hkl) planes was calculated by using the diffraction angle (2θ) measured by XRD and the wavelength of x-ray irradiated by Cu $K\alpha_1$ ($\lambda = 1.5406$ Å), through the following equation:

$$d = \frac{\lambda}{2sin\theta}. \qquad \text{(Eq. S1)}$$

The values of h, k, l for the lattice planes were calculated by using the unit cell data for the TTF-chlorides in Table S1, through the following equation:

$$\frac{1}{d^2} = \frac{h^2}{a^2} + \frac{k^2}{b^2} + \frac{l^2}{c^2} \,. \qquad \text{(Eq. S2)}$$

Unit Cell Data for TTF-Chlorides*	
Dication salts	a=13.56 c=10.10 *N*=8; *I4$_1$/acd*
Monocation salts	a=11.073 b=11.218 c=13.95 *N*=8; *PbCa*
Ordered mixed valence salts	a=10.77 b=3.56 c=22.10
Disordered mixed valence salts	a=11.12 c=3.595

* In Å units, maximum standard deviation ±0.05%. N is the number of formula units/cell.

Table S1. Unit cell data for TTF-chlorides.[1]

According to the unit cell data for TTF-chlorides in Table S1,[1] different crystal structures are identified.

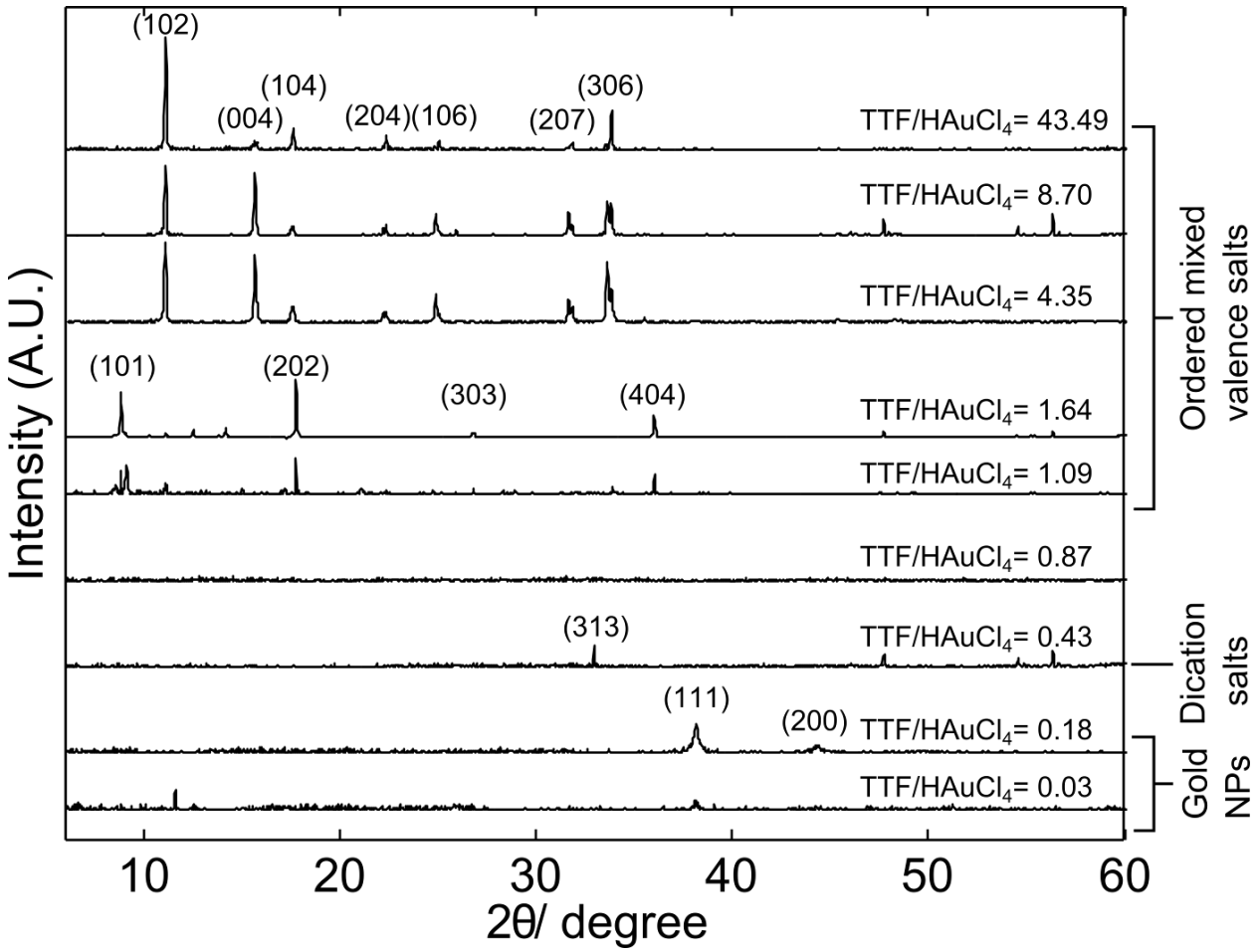

Figure S10. The XRD pattern of the samples synthesized by the bulk mixing method. The samples can be divided into 4 groups. (1) When the feed molar ratio TTF/$HAuCl_4$ ≤ 0.18, the samples show a primary peak corresponding to the face-centered cubic (fcc) structure of metallic gold, with the (111) diffraction intensified considerably. (2) When TTF/$HAuCl_4$ = 0.43, the (313) structure of $(TTF)Cl_2$ appears, indicating the presence of TTF^{2+}. (3) When TTF/$HAuCl_4$ = 0.87, no obvious peaks can be observed. (4) When TTF/$HAuCl_4$ ≥ 1.09, multiple peaks show the crystal structures of ordered mixed valence salt, indicating the presence of both TTF^{+} and TTF^{0}. When 1.09 ≤ TTF/$HAuCl_4$ ≤ 1.64, the (101) plane is the major crystal structure, resulting in the apex angle of 58º in the sample shapes. With the further increase in TTF/$HAuCl_4$, the (102) plane becomes the dominant plane.

When the feed molar ratio of TTF/$HAuCl_4$ ≤ 0.18 (corresponding to Fig. S8a-c), the XRD pattern showed sharp reflections corresponding to the face-centered cubic (fcc) structure of

metallic gold, with the (111) plane's reflection intensified considerably. This indicates that the structures in Fig. S9a-c were gold structures. This is a very common structural configuration in plate-like gold crystals such as gold nanoprisms or nanodisks.[2] As the molar ratio of TTF/$HAuCl_4$ increases to 0.43 (corresponding to Fig. S8d), the XRD results show (313) plane of the (TTF)Cl_2 crystals, indicating the presence of TTF^{2+}. This shows that the structures in Fig. S8d were (TTF)Cl_2 crystals. When the molar ratio of TTF/$HAuCl_4$ equals to 0.87 (corresponding to Fig. S8f), no diffraction peaks are present.

When the molar ratio of TTF/$HAuCl_4$ ranges between 1.09 and 1.64 (corresponding to Fig. S9a), the diffraction peak demonstrates the existence of (101) planes of the ordered mixed valence salts of TTF. According to Table S1, the (101) plane show 29º to the *c*-axis, which agrees well with the 58º apex angle of samples in Fig. S9a. With further increase in the molar ratio of TTF/$HAuCl_4$ (corresponding to Fig. S9b-c), the diffraction peak of (102) plane in the ordered mixed valence salts of TTF becomes dominant, indicating the fibers in Fig. S9b-c grew along (102) direction. When the molar ratio of TTF/$HAuCl_4$ < 8.7, another diffraction peak originated from (004) planes emerges, indicating the fibers were also with another top surface of (004) plane. When the molar ratio of TTF/$HAuCl_4$ increases to 43.49, the (102) diffraction peak becomes sharper, indicating that it is the dominant plane.

Size Distribution of Selected Samples

As shown in Fig. S11, during our experiments, 3D-HF can synthesize structures with better uniformity compared to the bulk mixing method. Table S2 compares the width distribution of the 1D structure formed by 3D-HF method and 2D-HF method, with the data of 2D-HF method from previous studies.[3]

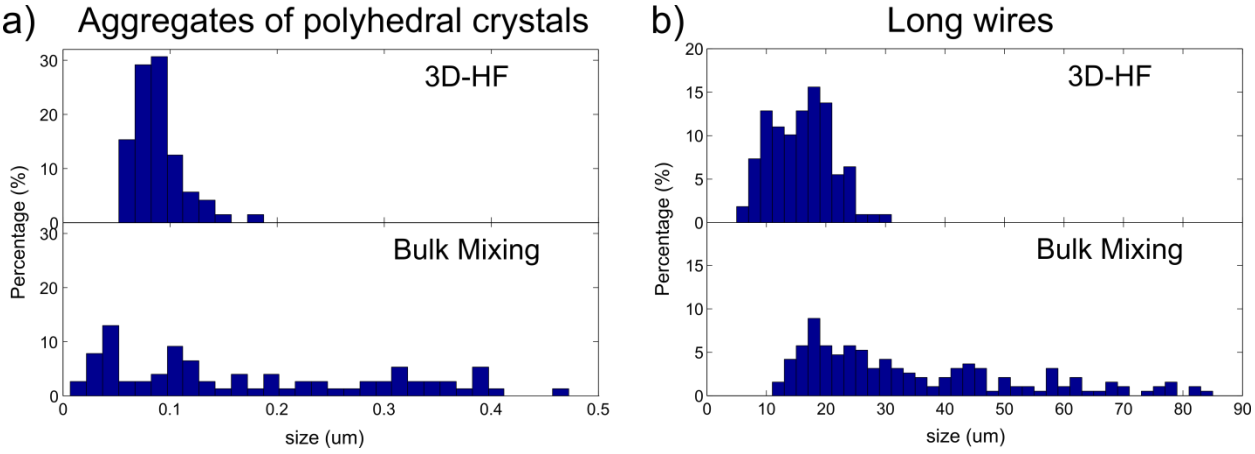

Figure S11. Size distribution of selected TTF-Au hybrid structures synthesized by 3D-HF and bulk mixing.

2D-HF		3D-HF	
Average width	Standard deviation	Average width	Standard deviation
0.17 μm	0.081 μm	0.15 μm	0.019 μm
0.38 μm	0.34 μm	0.40 μm	0.13 μm
0.93 μm	0.78 μm	0.97 μm	0.50 μm

Table S2. Width measurement of 1D TTF-Au hybrid structures synthesized by the 2D-HF method and the 3D-HF method. The average and standard deviations are calculated from approximately 100 different structures chosen randomly for each sample. The data for the 2D-HF method is obtained from previous studies.[3]

REFERENCES

(1) Scott, B. A.; La Placa, S. J.; Torrance, J. B.; Silverman, B. D.; Welber, B. The Crystal Chemistry of Organic Metals. Composition, Structure, and Stability in the Tetrathiafulvalinium-Halide Systems. *J. Am. Chem. Soc.* **1977**, *99*, 6631–6639.

(2) Shankar, S. S.; Rai, A.; Ankamwar, B.; Singh, A.; Ahmad, A.; Sastry, M. Biological Synthesis of Triangular Gold Nanoprisms. *Nat. Mater.* **2004**, *3*, 482–488.

(3) Puigmartí-Luis, J.; Schaffhauser, D.; Burg, B. R.; Dittrich, P. S. A Microfluidic Approach for the Formation of Conductive Nanowires and Hollow Hybrid Structures. *Adv. Mater.* **2010**, 22, 2255-2259.